ACS APPLIED MATERIALS & INTERFACES

Research Article

www.acsami.org

Au-Embedded ZnO/NiO Hybrid with Excellent Electrochemical Performance as Advanced Electrode Materials for Supercapacitor

Xin Zheng,[†] Xiaoqin Yan,*[,†] Yihui Sun,[†] Zhiming Bai,[†] Guangjie Zhang,[†] Yanwei Shen,[†] Qijie Liang,[†] and Yue Zhang*[,†,‡]

[†]State Key Laboratory for Advanced Metals and Materials, School of Materials Science and Engineering, University of Science and Technology Beijing, Beijing 100083, People's Republic of China

[‡]Key Laboratory of New Energy Materials and Technologies, University of Science and Technology Beijing, Beijing 100083, People's Republic of China

ABSTRACT: Here we design a nanostructure by embedding Au nanoparticles into ZnO/NiO core−shell composites as supercapacitors electrodes materials. This optimized hybrid electrodes exhibited an excellent electrochemical performance including a long-term cycling stability and a maximum specific areal capacitance of 4.1 F/cm^2 at a current density of 5 mA/cm^2, which is much higher than that of ZnO/NiO hierarchical materials (0.5 F/cm^2). Such an enhanced property is attributed to the increased electro−electrolyte interfaces, short electron diffusion pathways and good electrical conductivity. Apart from this, electrons can be temporarily trapped and accumulated at the Fermi level (EF′) because of the localized schottky barrier at Au/NiO interface in charge process until fill the gap between ZnO and NiO, so that additional electrons can be released during discharge. These results demonstrate that suitable interface engineering may open up new opportunities in the development of high-performance supercapacitors.

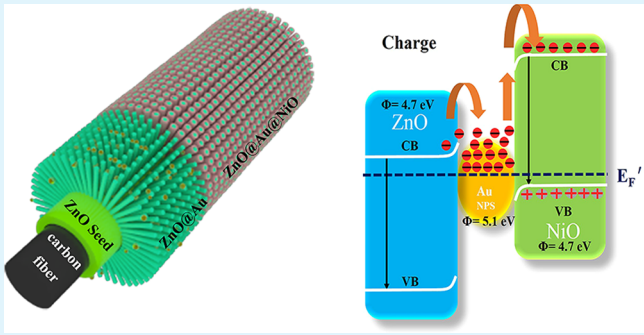

KEYWORDS: *interface engineering, supercapacitor, multishell, Au nanoparticles, electrons tapping effect*

INTRODUCTION

With the increasing power and energy demand of modern society and the emerging environmental concerns, it has become essential for the utilization of clean and renewable energy. Of the many available energy storage devices,[1−3] supercapacitors, also called electrochemical capacitors (ECs) or ultracapacitors, have attracted tremendous attentions owing to their significant superiorities such as high power density, fast charge/discharge rates and long cycle life in comparison to batteries and conventional dielectric capacitors. Numerous materials have been found to be suitable as the electrode materials in supercapacitors and can be classified into three types: carbonaceous materials,[4,5] conducting organic polymers[6,7] and transition metal oxides/hydroxides.[8,9] Commonly, NiO,[6] RuO_2,[10] $NiCoS_4$,[11] MnO_2,[12] Co_3O_4,[13] and $CoMoO_4$[14] have been widely used as the pseudocapacitors electrode materials. They have presented good capacitive performance. Among the transition metal oxides,[10−16] NiO has been widely investigated as candidate for supercapacitors with low cost, high theoretical capacity (2573 F g^{-1}) and high power density.[17−20] However, the low surface area and poor electrical conductivity of NiO limit its wide application as high-performance supercapacitors.

To overcome this problem, three-dimensional nanostructured electrodes have been extensively researched to shorten diffusion distance of electrolytes into pseudocapacitor electrodes.[21,22] 3D ZnO nanowire/nanorod combined with several transition metal oxides used for pesudocapacitors have been developed to enhance the electrochemical behavior.[23−28] These studies proved that the remarkable performance was because that ZnO worked as a conducting scaffold for supporting electrochemically active materials and an effective channel for electrons transport.[29] In addition, ZnO nanowire could function as efficient mechanical support because of high chemical stability and mechanical flexibility,[30] which is expected to be a promising high-performance electrode material for flexible supercapacitors.

It is well-known that gold nanoparticles supported on metal oxides have proven to be highly active and selective catalysts for various chemical reactions.[31] Another hopeful advantage of gold is its good conductivity, which is helpful to electron transfer. Recently, compounding conductive Au and Ag on metal oxide pseudocapacitor electrodes was also demonstrated to be another effective strategy to improve rate performance.[32,33]

In this work, we report an optimized supercapacitor electrode material based on 3D ZnO−NiO composites by incorporation of very small amounts of Au nanoparticles, the

Received: October 23, 2014
Accepted: January 13, 2015
Published: January 13, 2015

DOI: 10.1021/am5073468
ACS Appl. Mater. Interfaces 2015, 7, 2480−2485

resultant electrode exhibited ultraperformance with high specific areal capacitance of 4.1 F/cm^2 at a current density of 5 mA/cm^2 and good cycling stability, which is truly superior to the ZnO−NiO core−shell nanomaterials. The decorated Au nanoparticles not only accelerated electron conduction but also temporarily trapped and accumulated electrons resulting in more electrons release in discharge process. Band theory were further utilized to account for improved capacitive performance of the ZnO−Au−NiO. Our study provides that the suitable interface design can be used for enhancing the efficiency of energy storage devices.

EXPERIMENTAL SECTION

Synthesis of ZnO−Au−NiO Composites. Briefly, the carbon cloth (WOS1002, 1 cm × 1 cm × 360 μm) was first cleaned ultrasonically in acetone, ethanol, and deionized water for 10 min, respectively. The carbon cloth was dipped in ethanol solution of 0.1 M zinc acetate to form a seed layer. Then the carbon cloth was dried at 100 °C for 10 min and sintered at 350 °C for 15 min for 3−4 times to ensure complete coverage of the carbon cloth with a ZnO seed layer.[34] A 100 mL precursor solution was prepared with 0.015 M of zinc nitrate hexahydrate and 0.015 M of hexamethylenetetramine (HMTA) added with 4 mL of ammonia. The carbon cloth was placed in the precursor solution under 90 °C for 15 h.

Au NPs was synthesized by photoreduction method[35] and deposited in situ onto the ZnO NR arrays by the following procedures. First, 0.05% $HAuCl_4$ aqueous solution, 1% poly(vinyl alcohol) (PVA) solution, and methanol were mixed together with a proper ratio. The pH value of the mixed solution was adjusted to 8 by NaOH. When Au NPs protected by PVA were negatively charged while ZnO NR arrays were positively charged. The carbon cloth with ZnO NR arrays was then immersed in the photoreduction solution and an ultravitalux lamp (OSRAM, 300 W) was used to irradiate 15 min for the photoreduction. Next, ZnO arrays attached with Au nanoparticles were annealed in air at 350 °C for 0.5 h to remove the capped PVA.

NiO nanosheets were prepared by chemical bath deposition (CBD) in previous study.[19] The solution for the CBD was obtained by mixing 40 mL of 1 M nickel sulfate, 30 mL of 0.25 M potassium persulfate, and 10 mL of aqueous ammonia in a 100 mL beaker at room temperature. The ZnO−Au composites were placed vertically in the fresh resulting solution, kept at 25 °C for 30 min and then subjected to calcination at 350 °C for 1.5 h.

Characterization and Measurements. Small pieces of the samples were tailored and pasted onto aluminum metal table with conductive adhesives for scanning electron microscopy (FESEM, FEI Quanta 3D) observations. The ZnO−Au−NiO samples were removed from carbon cloth surface into alcohol solution during ultrasonic dispersion. Then the alcohol solution with ZnO-Au-NiO samples was dropped onto copper net with support film for transmission electron microscopy (JEOL, JEM-2010) characterization. X-ray diffraction patterns were carried out at room temperature using a Rigaku DMA-RB X-ray diffractometer with an incident X-ray beam (λ = 1.5406 Å) at 40 kV and 30 mA with Cu-Ka radiation. Energy dispersive spectrometer (EDS) measurements were performed to evaluate the structure and element properties. Surface elements of electron materials were investigated by X-ray photoelectron spectroscopy (AXIS ULTRADLD), using Al Kα ($h\nu$ = 1486.6 eV) as an exciting X-ray source.

Electrochemical Measurements. Cyclic voltammetry (CV), galvanostatic charge−discharge and impedance measurements were carried out in a conventional three-electrode configuration at room temperature by an electrochemical workstation (SI 1287, Solartron Analytical). The synthesized electrode on the textile substrate acted as a working electrode. Ag/AgCl electrode and platinum foil served as reference and counter electrodes, respectively. Electrochemical impedance spectroscopy (EIS) was performed in the frequency range from 100 kHz at open circuit voltage by applying a 5 mV signal. All electrochemical measurements were carried out in 1.0 mol L^{-1} KOH electrolyte.

RESULTS AND DISCUSSION

The formation process is schematically shown in Figure 1a. First, ZnO nanoarrays were grown directly on carbon cloth by a simple hydrothermal method.[34,36] Afterward, small amounts of Au nanoparticles were synthesized to coat the ZnO nanowires and NiO nanosheets were in situ deposited on the surface of Au-modified ZnO nanowires resulting in ZnO−Au−NiO core−shell hierarchitectures. Figure 1b shows the typical SEM images of the ZnO nanorods. It can been clearly seen that large area ZnO nanorod arrays were grown continuously on carbon cloth substrates. The diameter and the length of the ZnO nanorod are 200−300 nm and 3 μm, respectively, and very small amounts of Au nanoparticles have been introduced in the sample (Figure 1c). The intermediate products were further covered by NiO nanosheets. The SEM views of the final samples indicated in Figure 1d suggest that numerous NiO nanoflakes with a thickness of about dozens of nanometers were deposited uniformly on the surface of ZnO nanowire and fill the space in between.

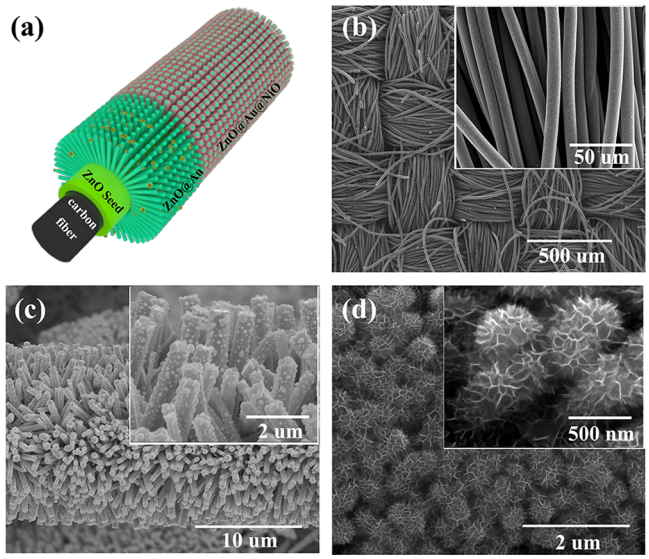

Figure 1. Schematic illustration of the fabrication process for three-dimensional NiO@Au@ZnO hybrid nanostructure (a). SEM images of ZnO nanorods and its corresponding enlarged image on carbon cloth (b), ZnO nanorods modified by Au nanoparticles at different resolutions (c), and the low and high magnification images of the ZnO−Au−NiO hybrid composites (d).

Additionally, energy dispersive spectroscopy (EDS) showing the presence of the corresponding elements of Zn, Au, Ni, and O (as shown in Figure 2a). XRD measurements was evaluated to identify the phase and composition of the as-prepared samples (see Figure 2b). Obviously, the XRD pattern exhibited corresponding patterns from pure ZnO to ZnO/Au/NiO composites. The single-crystal NiO nanosheet and Au nanoparticles are both cubic phase, ZnO nanorods associated with the wurtzite phase. According to the Scherrer's equation

$$D_{hkl} = k\lambda/\beta \cos\theta \quad (1)$$

where k is Scherrer constant with the value of 0.89, λ is the X-ray wavelength with the value of 0.15406 nm, β is full width half-maximum with the value of 0.305 min, and θ is incident

DOI: 10.1021/am5073468
ACS Appl. Mater. Interfaces 2015, 7, 2480−2485

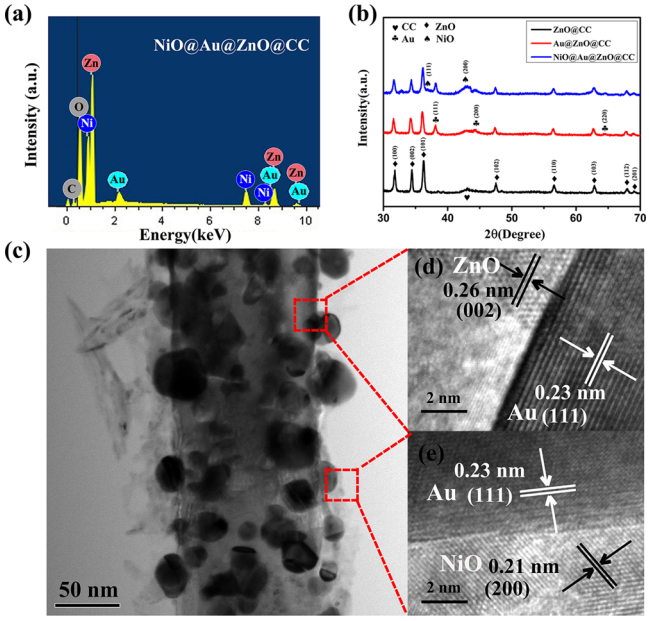

Figure 2. (a) EDS spectrum of the ZnO@Au@NiO product. (b) XRD patterns of the samples at different preparation stages. (c) TEM images of ZnO@Au@NiO core−shell nanostructure and (d and e) the corresponding HRTEM images.

angle with the value of 19.09°. The mean crystallite size of the Au nanoparticles is 27.27 nm. As for NiO nanosheets, the full width half-maximum is 0.716 min and the incident angle is 21.63°. By calculatiion, the NiO nanosheets have the thickness of 11.8 nm. These agree well with the TEM and SEM results. No peaks from other phases existed, indicating the high purity of the obtained electrode materials.

The as-prepared products were further characterized by TEM (Figure 2c−e). The TEM observation was consistent with the SEM observation. ZnO nanowires were fully covered with few Au nanoparticles and thin NiO nanosheets, forming a typical 3D architecture. Further information was presented in high resolution TEM (HRTEM) image (Figure 2d), which displayed a distinct ZnO (002) plane spacing of 0.26 nm, Au (111) plane spacing of 0.23 nm, and visible lattice fringes with an equal interplanar distance of 0.21 nm, corresponding to the (200) plane of face-centered cubic phase NiO, respectively. This is in good agreement with the XRD analysis (Figure 2b).

Figure 3 displayed the XPS spectra of this hybrid electrode. The appearance of two peaks centered at 1022.5 and 1045.5 eV can be assigned to Zn $2p_{3/2}$ and Zn $2p_{1/2}$ (Figure 3a), respectively. In Figure 3b, it can been observed that two Au 4f binding-energy peaks at 83.8 and 87.4 eV, which is reported previously. Figure 3c gives the XPS spectra of the Ni 2p. The main peaks located at 855.5, 873.8, 861.7, 880.0 eV are corresponding to Ni═O $2p_{3/2}$, $2p_{1/2}$, and its satellites respectively, suggesting the Ni^{2+} ions are dominant in the product.

Further insights into the electrochemical properties of the electrode materials were achieved by electrochemical measurements of ZnO/Au/NiO composites in a three-electrode electrochemical cell containing a 1 M KOH as the electrolyte. At first, cyclic voltammetry (CV) was tested at 2 mVs^{-1} within the potential range of 0−0.50 V (vs SCE). To explore the exceptional specific capacitance contribution from Au nanoparticles, ZnO/NiO core−shell composites were prepared to act as comparative electrodes. It turns out that ZnO/Au/NiO electrodes possess larger areas in the CVs indicating the higher level of stored charge and performing better electrochemical behavior than ZnO/NiO nanorods. Faradaic reactions corresponding to the redox peaks are as follows:

$$NiO + OH^{-1} \leftrightarrow NiOOH + e^{-1} \quad (2)$$

As shown in Figure 4b, galvanostatic charge−discharge measurements were subsequently tested to estimate the specific capacitance of electrode materials in the voltage range between 0 and 0.5 V at 2 $mAcm^{-2}$. The corresponding specific

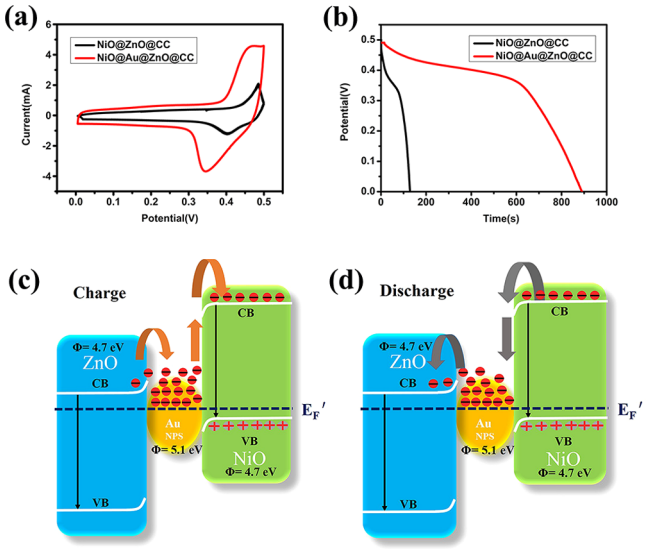

Figure 4. (a) CV curves of ZnO@Au@NiO and ZnO@NiO electrodes measured at 2 mVs^{-1}. (b) Galvanostatic discharge curves of ZnO@Au@NiO and ZnO@NiO electrodes collected at a current density of 2 $mAcm^{-2}$. (c, d) The energy level diagram at the interface of ZnO−Au and NiO−Au in charge/discharge process, indicating Au nanoparticles produce an electrons trapping channel.

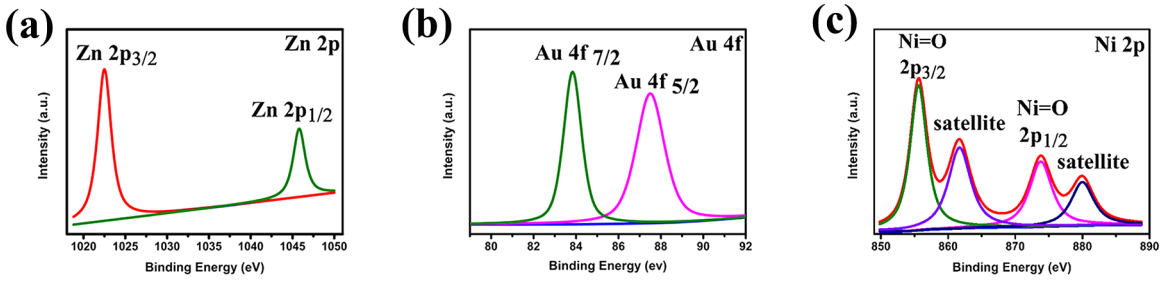

Figure 3. XPS spectra of (a) Zn 2p, (b) Au 4f, and (c) Ni 2p for the composites.

DOI: 10.1021/am5073468
ACS Appl. Mater. Interfaces 2015, 7, 2480−2485

capacitance can been expressed using the eqs 2, By calculation, the areal capacitance of the ZnO@Au@NiO nanocomposite is 3.50 F/cm^2 at the current density of 2 mAcm^{-2}, whereas the ZnO@NiO electrodes only display 0.42 F/cm^2.

Consequently modifying Au nanoparticles is an effective method in boosting the performance of the supercapacitors electrodes.

$$C_s = \frac{it}{m\Delta V} \quad (3)$$

It is obvious that the peak of the ZnO−Au−NiO composites shifts much compared to that of ZnO−NiO hybrid (Figure 4a), the negative shift of the onset potential of the oxidation reaction is attributed to two factors: On one hand, a decreased energy barrier would be required for the NiO/NiOOH reaction resulting in the improvement in the reaction kinetics and the better electrochemical activities of the NiO. The enhanced electrochemical activities of the ZnO−NiO composites combined with Au nanoparticles could be ascribed to the larger surface area of NiO nanosheets and the improved conductivity of the NiO, which may lead to higher current intensities of the redox couple and lower onset potential of the oxidation reaction. On the other hand, electrons can be temporarily trapped and accumulated at the Fermi level (EF) due to the localized schottky barrier at Au/NiO interface in charge process until fill the gap between ZnO and NiO (Figure 4c), so that additional electrons can be released during discharge (Figure 4d). As a result, an additional current density exists before the NiO/NiOOH reaction in the CV curves and larger capacitance can been obtained.

Figure 5b plotted the changes in the relative specific capacitance of the ZnO/Au/NiO electrodes depending on

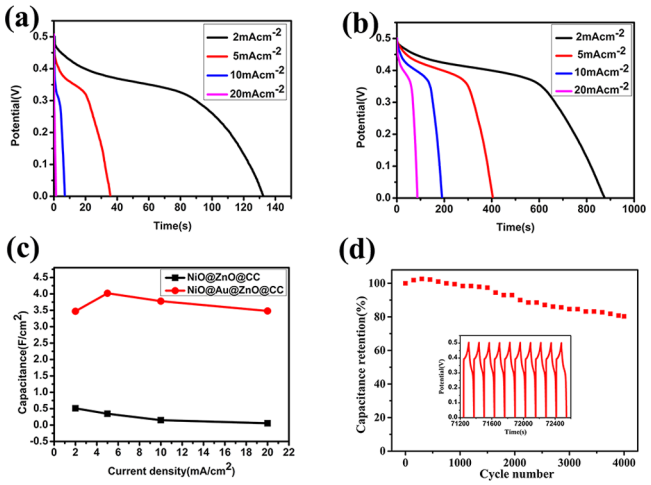

Figure 5. (a, b) Galvanostatic discharge curves for ZnO−NiO and ZnO−Au−NiO electrode at various current densities of 2, 5, 10, and 20 mA cm^{-2}, respectively. (c) A comparison of the specific capacitance of two electrodes. (d) Cycling stability of the ZnO/Au/NiO electrodes at 30 mA cm^{-2} in 1 M KOH electrolyte as a function of cycle numbers.

various current densities from 2 to 20 mA cm^{-2}. For comparison, corresponding galvanostatic charge−discharge curves of ZnO@NiO are provided (Figure 5a). According to eq 3, the area capacitance of the two electrodes can be calculated and depicted in Figure 5c. Obviously, our approach inserts very small amounts of Au nanoparticles into ZnO/NiO core−shell structure resulting in dramatic improvements of the electrochemical properties. The decorated Au nanoparticles can accelerate electron transportation and electrons can been accumulated at Au nanoparticles/NiO interfacial resulting in more electrons release in discharge process. This interface engineering design can also been utilized to improve capacitive performance of other active oxides electrode materials.

As is known to all, a long cycle life is one of the key factors for supercapacitors application, an endurance test based on ZnO@Au@NiO structure was conducted by galvanostatic charge−discharge test at 30 mAcm^{-2}. Before the initial 450 cycles, a small increase of capacitance was observed, this phenomenon may be due to an activation process occurring at the beginning of the charging/discharging cycling test. With the electrolyte gradually penetrating into the electrode, more and more electrode material is activated, thus contributing to the increase in the specific capacitance[37] (Figure 5d). And then the capacitance tends to slowly decrease, the electrode material maintained about 80.3% of the original capacitance after 4000 cycles, implying this electrode fabricated shows a good cyclic stability.

To further confirm the role of Au nanopaticles in electron transport process, the measured EIS results show a single semicircles over the high frequency range, followed by the short straight lines in the low-frequency region for the two samples (Figure 6). The diameter of the semicircle corresponds to the

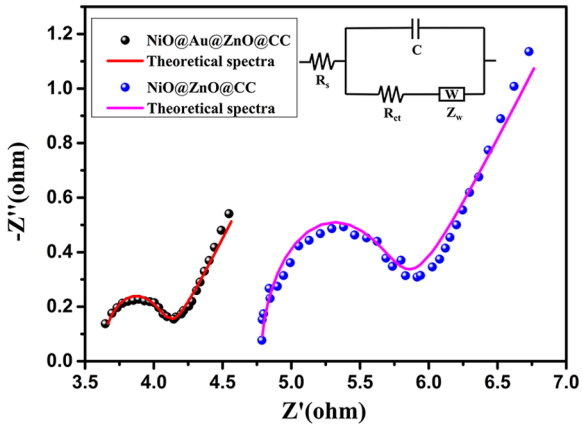

Figure 6. Electrochemical impedance spectra (EIS) of ZnO−NiO with Au nanoparticles or not in the frequency range from 10 mHz to 100 kHz in 1 KOH solution.

interfacial charge-transfer resistance (R_{ct}), which usually represents the resistance of electrochemical reactions on the electrode. The R_{ct} for ZnO−NiO and ZnO−Au−NiO composites are calculated as 0.963 and 0.468 Ω respectively. The charge-transfer resistance (Rct) decreases obviously as the Au nanoparticles introduced, which indicates Au nanoparticle can promote the electron transportation between ZnO and NiO. And the Schottky junction at the ZnO−NiO interface does not lead to a large increase in resistance. Therefore, the enhanced pseudocapacitance behavior is also attributed to the higher electron transfer rate assisted by Au nanopaticles.

CONCLUSION

In summary, 3D ZnO−NiO hybrid architectures have been synthesized for supercapacitor electrodes with Au nanopaticles implanted at the interface between ZnO nanorods and NiO nanosheets. The ZnO−Au−NiO composites exhibited the maximum specific capacitance of 4.1 F/cm^2 at current density

DOI: 10.1021/am5073468
ACS Appl. Mater. Interfaces 2015, 7, 2480−2485

of 5 $mAcm^{-2}$ and excellent stability (about 19.7% loss after 4000 cycles), which is not only because of the low internal resistance but also due to electrons tapping and accumulation effect of Au nanopaticles/NiO interfacial schottky barrier. It is demonstrated that the ZnO−Au−NiO core−shell structure is a promising candidate for application in efficient energy storage devices and interface engineering design may open up new opportunities in the development of high-performance supercapacitors.

AUTHOR INFORMATION

Corresponding Authors

*E-mail: yuezhang@ustb.edu.cn.

*E-mail: xqyan@mater.ustb.edu.cn.

Notes

The authors declare no competing financial interest.

ACKNOWLEDGMENTS

This work was supported by the National Major Research Program of China (2013CB932602), the Major Project of International Cooperation and Exchanges (2012DFA50990), the Program of Introducing Talents of Discipline to Universities, NSFC (51232001, 51172022, 51372023, 51372020), the Research Fund of Co-construction Program from Beijing Municipal Commission of Education, the Fundamental Research Funds for the Central Universities, the Program for Changjiang Scholars and Innovative Research Team in University.

REFERENCES

(1) Xin, S.; Yin, Y.; Guo, Y.; Wan, L. J. A High-Energy Room-Temperature Sodium-Sulfur Battery. *Adv. Mater.* **2014**, *26*, 1261−1265.

(2) Mo, R.; Lei, Z.; Sun, K.; Rooney, D. Facile Synthesis of Anatase TiO_2 Quantum-Dot/Graphene-Nanosheet Composites with Enhanced Electrochemical Performance for Lithium-Ion Batteries. *Adv. Mater.* **2014**, *26*, 2084−2088.

(3) Chabi, S.; Peng, C.; Hu, D.; Zhu, Y. Ideal Three-Dimensional Electrode Structures for Electrochemical Energy Storage. *Adv. Mater.* **2014**, *26*, 2440−2445.

(4) Beguin, F.; Presser, V.; Balducci, A.; Frackowiak, E. Carbons and Electrolytes for Advanced Supercapacitors. *Adv. Mater.* **2014**, *26*, 2219−2251.

(5) Cai, X.; Peng, M.; Yu, X.; Fu, Y.; Zou, D. Flexible Planar/Fiber-Architectured Supercapacitors for Wearable Energy Storage. *J. Mater. Chem. C* **2014**, *2*, 1184−1200.

(6) Shin, D.; Lee, J.; Jun, J.; Jang, J. Fabrication of Amorphous Carbon-Coated NiO Nanofibers for Electrochemical Capacitor Applications. *J. Mater. Chem. A* **2014**, *2*, 3364−3371.

(7) Inganas, O.; Admassie, S. 25th Anniversary Article: Organic Photovoltaic Modules and Biopolymer Supercapacitors for Supply of Renewable Electricity: A Perspective from Africa. *Adv. Mater.* **2014**, *26*, 830−848.

(8) Augustyn, V.; Simon, P.; Dunn, B. Pseudocapacitive Oxide Materials for High-Rate Electrochemical Energy Storage. *Energy Environ. Sci.* **2014**, *7*, 1597−1614.

(9) Chang, H.; Kang, J.; Chen, L.; Wang, J.; Ohmura, K.; Chen, N.; Fujita, T.; Wu, H.; Chen, M. Low-Temperature Solution-Processable $Ni(OH)_2$ Ultrathin Nanosheet/N-graphene Nanohybrids for High-Performance Supercapacitor Electrodes. *Nanoscale* **2014**, *6*, 5960−5966.

(10) Wu, Z.; Wang, D.; Ren, W. Anchoring Hydrous RuO_2 on Graphene Sheets for High-Performance Electrochemical Capacitors. *Adv. Funct. Mater.* **2010**, *20*, 3595−3602.

(11) X, J.; Wan, L.; Yang, S.; Xiao, F.; Wang, S. Design Hierarchical Electrodes with Highly Conductive $NiCo_2S_4$ Nanotube Arrays Grown on Carbon Fiber Paper for High-Performance Pseudocapacitors. *Nano Lett.* **2014**, *14*, 831−838.

(12) Chen, Y.; Chen, P.; Chen, T.; Lee, C.; Chiu, H. Nanosized MnO_2 Spines on Au Stems for High-Performance Flexible Supercapacitor Electrodes. *J. Mater. Chem. A* **2013**, *1*, 13301−13307.

(13) Rakhi, R.; Chen, W.; Cha, D.; Alshareef, H. Substrate Dependent Self-Organization of Mesoporous Cobalt Oxide Nanowires with Remarkable Pseudocapacitance. *Nano Lett.* **2012**, *12*, 2559−2567.

(14) Yu, X.; Lu, B.; Xu, Z. Super Long-Life Supercapacitors Based on the Construction of Nanohoneycomb-Like Strongly Coupled $CoMoO_4$−3D Graphene Hybrid Electrodes. *Adv. Mater.* **2014**, *26*, 1044−1051.

(15) Cheng, K.; Yang, F.; Ye, K.; Li, Y.; Yang, S.; Yin, J.; Wang, G.; Cao, D. Facile Preparation of Transition Metal Oxide−Metal Composites with Unique Nanostructures and Their Electrochemical Performance as Energy Storage Material. *J. Mater. Chem. A* **2013**, *1*, 14246−14252.

(16) Wang, Y.; Lei, Y.; Li, J.; Gu, L.; Yuan, H.; Xiao, D. Synthesis of 3D-Nanonet Hollow Structured Co_3O_4 for High Capacity Supercapacitor. *ACS Appl. Mater. Interfaces* **2014**, *6*, 6739−6747.

(17) Qian, Y.; Liu, R.; Wang, Q.; Xu, J.; Chen, D.; Shen, G. Efficient Synthesis of Hierarchical NiO Nanosheets for High-Performance Flexible All-Solid-State Supercapacitor. *J. Mater. Chem. A* **2014**, *2*, 10917−10922.

(18) Yang, Z.; Xu, F.; Zhang, W.; Mei, Z.; Pei, B.; Zhu, X. Controllable Preparation of Multishelled NiO Hollow Nanospheres via Layer-By-Layer Self-assembly for Supercapacitor Application. *J. Power Sources* **2014**, *246*, 24−28.

(19) Huang, M.; Gu, C.; Ge, X.; Wang, X.; Tu, J. NiO Nanoflakes Grown on Porous Graphene Frameworks as Advanced Electrochemical Pseudocapacitor Materials. *J. Power Sources* **2014**, *259*, 98−105.

(20) Zhou, M.; Chai, H.; Jia, D.; Zhou, W. The Glucose-Assisted Synthesis of a Graphene Nanosheet−NiO Composite for High-performance Supercapacitors. *New J. Chem.* **2014**, *46*, 254−230.

(21) Ellis, B.; Knauth, L. Three-Dimensional Self-Supported Metal Oxides for Advanced Energy Storage. *Adv. Mater.* **2014**, *26*, 3368−3397.

(22) Qiu, Y.; Zhao, Y.; Yang, X.; Li, W.; Wei, Z.; Xiao, J.; Leung, S.; Lin, Q.; Wu, H.; Zhang, Y.; Fan, Z.; Yang, S. Three-Dimensional Metal/Oxide Nanocone Arrays for High-performance Electrochemical Pseudocapacitors. *Nanoscale* **2014**, *6*, 3626−3631.

(23) Chao, D.; Xia, X.; Zhu, C.; Wang, J.; Liu, J.; Lin, J.; Shen, Z.; Fan, H. J. Hollow Nickel Nanocorn Arrays as Three-Dimensional and Conductive Support for Metal Oxides to Boost Supercapacitive Performance. *Nanoscale* **2014**, *6*, 5691−5697.

(24) Xia, X.; Tu, J.; Zhang, Y.; Wang, X.; Gu, C.; Zhao, X.; Fan, H. High-Quality Metal Oxide Core/Shell Nanowire Arrays on Conductive Substrates for Electrochemical Energy Storage. *ACS Nano* **2012**, *6*, 5531−5538.

(25) Li, N.; Wang, J.-Y.; Liu, Z.-Q.; Guo, Y.-P.; Wang, D.-Y.; Su, Y.-Z.; Chen, S. One-Dimensional ZnO/Mn_3O_4 Core/Shell Nanorod and Nanotube Arrays with High Supercapacitive Performance for Electrochemical Energy Storage. *RSC Adv.* **2014**, *4*, 17274−17281.

(26) Li, S.; Wen, J.; Mo, X.; Long, H.; Wang, H.; Wang, J.; Fang, G. Three-Dimensional MnO_2 Nanowire/ZnO Nanorod Arrays Hybrid Nanostructure for High-Performance and Flexible Supercapacitor Electrode. *J. Power Sources* **2014**, *256*, 206−211.

(27) Pu, Z.; Liu, Q.; Qusti, A.; Asiri, A.; Al-Youbi, A.; Sun, X. Fabrication of $Ni(OH)_2$ Coated ZnO Array for High-Rate Pseudocapacitive Energy Storage. *Electrochim. Acta* **2013**, *109*, 252−255.

(28) Cai, D.; Huang, H.; Wang, D.; Liu, B.; Wang, L.; Liu, Y.; Li, Q. High-Performance Supercapacitor Electrode Based on the Unique $ZnO@Co_3O_4$ Core/Shell Heterostructures on Nickel Foam. *ACS Appl. Mater. Interfaces* **2014**, *6*, 15905−15912.

(29) Zheng, X.; Sun, Y.; Yan, X.; Chen, X.; Bai, Z.; Zhang, Y. Tunable Channel Width of A UV-Gate Field Effect Transistor Based on ZnO Micro-Nano Wire. *RSC Adv.* **2014**, *4*, 18378−18381.

DOI: 10.1021/am5073468
ACS Appl. Mater. Interfaces 2015, 7, 2480−2485

(30) Li, W.; Li, G.; Sun, J.; Zou, R.; Xu, K.; Sun, Y.; Chen, Z.; Yang, J.; Hu, J. Hierarchical Heterostructures of MnO_2 Nanosheets or Nanorods Grown on Au-Coated Co_3O_4 Porous Nanowalls for High-Performance Pseudocapacitance. *Nanoscale* **2013**, *5*, 2901−2908.
(31) Zhang, Y.; Yan, X.; Yang, Y.; Huang, Y.; Liao, Q.; Qi, J. Scanning Probe Study on the Piezotronic Effect in ZnO Nanomaterials and Nanodevices. *Adv. Mater.* **2012**, *24*, 4647−4655.
(32) Bauer, J.; Toops, T.; Oyola, Y.; Ii, J.; Dai, S.; Overbury, S. Catalytic Activity and Thermal Stability of Au−CuO/SiO_2 Catalysts for the Low Temperature Oxidation of CO in the Presence of Propylene and NO. *Catal. Today* **2014**, *231*, 15−21.
(33) Lu, X.; Zhai, T.; Zhang, X.; Shen, Y.; Yuan, L.; Hu, B.; Gong, L.; Chen, J.; Wang, Z. WO_{3-x}@Au@MnO_2 Core−Shell Nanowires on Carbon Fabric for High-Performance Flexible Supercapacitors. *Adv. Mater.* **2012**, *24*, 938−944.
(34) Liao, Q.; Mohr, M.; Zhang, X.; Zhang, Z.; Zhang, Y.; Fecht, H. Carbon Fiber−ZnO Nanowire Hybrid Structures for Flexible and Adaptable Strain Sensors. *Nanoscale* **2013**, *5*, 12350−12355.
(35) Sau, A.; Jana, N.; Wang, Z.; Pal, T. Size Controlled Synthesis of Gold Nanoparticles using Photochemically Prepared Seed Particles. *J. Nanopart. Res.* **2001**, *3*, 257−261.
(36) Yang, P.; Xiao, X.; Li, Y.; Ding, Y.; Qiang, P.; Tan, X.; Mai, W.; Lin, Z.; Wu, W.; Li, T.; Wang, Z. Hydrogenated ZnO Core-Shell Nanocables for Flexible Supercapacitors and Self-Powered Systems. *ACS Nano* **2013**, *7*, 2617−2626.
(37) Xia, X.; Tu, J.; Zhang, Y.; Wang, X.; Gu, C.; Fan, H. J. High-Quality Metal Oxide Core/Shell Nanowire Arrays on Conductive Substrates for Electrochemical Energy Storage. *ACS Nano* **2012**, *6*, 5531−5538.

DOI: 10.1021/am5073468
ACS Appl. Mater. Interfaces 2015, 7, 2480−2485